Small slope approximation method : Higher order contributions for scattering from conducting 3D surfaces

Gérard Berginc[a], Yannick Béniguel[b], Bruno Chevalier[a]

[a] Thomson-CSF Optronique, 78283 Guyancourt Cedex France
[b] IEEA 13, promenade Paul Doumer, 92400 Courbevoie France

ABSTRACT

The analysis presented in this paper focuses on the calculation of the scattering cross-section of randomly rough canonical three-dimensional objects. The scattering cross-section of objects is calculated by the Small Slope Approximation (SSA) method. The SSA method was suggested by Voronovich. The small parameter of the method, the roughness slope, differs from those used in classical approaches since it is independent of the incident electromagnetic wavelength. Second-order terms in SSA method have been implemented in order to obtain accurate results for a large range of slopes. Specific developments have been carried out for the TM case which presents a singularity. In this paper we discuss the theoretical SSA solution. Calculations are presented for both polarizations of the electromagnetic field. Numerical simulations with higher order contributions of SSA method and comparisons with published results will be discussed in this paper.

Keywords: Randomly rough scattering, surface scattering, scattering cross-section, small slope approximation, numerical simulations.

1. INTRODUCTION

Much research has been done on the problem of wave scattering from randomly rough surfaces because of many applications in underwater acoustics, optics, radiophysics, radioastronomy and solid state physics. Two approaches were suggested [1,2].
One is related to the development of numerical methods of calculating the diffraction wave fields from surfaces of a given shape. These methods consider different approaches of constructing a set of linear equations and solving them numerically. Computers allow now to solve problems of scattering from randomly rough surfaces, i.e. numerical calculations for statistical ensembles of roughness. But numerical simulations do not answer all questions : when we consider a three-dimensional problem, dimensions of sets of linear equations can be too large.
The second approach concerns the development of theoretical analytic methods describing scattering of electromagnetic or acoustic waves by rough surfaces both in deterministic and statistical cases. But the scattering problem for rough surface has no analytic exact solution for rough surface. Only approximate analytic solutions to this problem exist. Two basic methods were used before: the perturbation method which is valid for small values of the Rayleigh parameter, the ratio of roughness height to the incident wavelength, and the Kirchhoff approximation which is valid for small values of the ratio of wavelength to curvature radius of the surface. In the Kirchhoff approximation, the boundary can be approximated at each point by a tangent plane, this theory assumes that the interaction of the acoustic or electromagnetic wave with the roughness is local. These two classical approaches are useful, but they depend on the way how the rough surface is described, i.e., large or small scale of roughness. A combination of these different methods, called the two-scale approach, is also used. But this model is inacurate for grazing angle scattering.
Two new approaches were suggested, one proposed by Voronovich[3,4], the other proposed by Bahar[5,6]. The aim of these approaches is to develop a scattering theory which reduces to both classical theories when they are accurate. These approaches eliminate the composite roughness approach. Voronovich's theory describes randomly-rough-scattering on the basis of a small parameter which is the roughness slope. In the case of a randomly rough surface, this small parameter is defined as the ratio of the surface root mean square (RMS) height to the surface correlation length. The small slope approximation is formulated as a series which is an expansion in power of slope.
In this paper, we examine the Small Slope Approximation of Voronovich. In the first part of the paper, we present the calculation of the first- and second-order of the small slope approximation. We consider polarized electromagnetic wave: TE case and TM case. Second order terms are implemented in order to obtain accurate results for a large range of slopes. Therefore the SSA method applies not only to small slope profiles but also to significant values of slope. We consider a perfectly conducting surface. In the second part of the paper, scattered field intensity and bistatic radar cross sections for

both TE and TM polarizations are calculated using the second order of the small slope approximation. The problem is limited to vector-wave scattering from three-dimensional randomly rough conducting surfaces with a Gaussian roughness spectrum. We consider the 3-D scattering problem. Some refinements are made for the TM case and specific developments are carried out for the TM polarization case since this case presents a singularity. In this part, we give a detailed derivation of the calculation of the scattered field intensity for TE and TM cases. In the third part of the paper, numerical results for scattering cross-section of randomly rough conducting plates for TE and TM cases are given using the second order of the small slope approximation. Comparisons with the full-wave method of Bahar are presented. Finally, in the last part we attempt to give some insight into the calculation of the monostatic laser radar cross-section of more complex objects with randomly rough conducting surfaces.

2. SMALL SLOPE APPROXIMATION METHOD

The Small Slope Approximation gives a solution for wave scattering both at small and large scales within the single theoretical scheme provided that surface roughness has small slopes. In this part of the paper, we describe the small slope approximation method. A monochromatic plane wave of pulsation ω is incident on the rough boundary. We assume that ($\mathbf{r}$,z) are the horizontal and vertical coordinates of an observation point, and that ($\mathbf{k}$, $q_{\mathbf{k}}$), with $q_{\mathbf{k}} = (K^2 - \mathbf{k}^2)^{1/2}$ (Im q $\geq$ 0) and K=ω/c, are the horizontal and vertical components of the wavevector. We can notice that $\mathbf{r}$ and $\mathbf{k}$ are vectors. The wavevectors in the incident and scattered directions are respectively given by $k_o\,\hat{\mathbf{r}} + q_{\mathbf{o}}\,\hat{\mathbf{z}}$ and $k\,\hat{\mathbf{r}} - q_{\mathbf{k}}\,\hat{\mathbf{z}}$, where $\hat{\mathbf{r}}$ and $\hat{\mathbf{z}}$ are unitary vectors. The z-axis is directed downwards. The index 'o' specifies the incident wave $\left(q_{\mathbf{0}} = q_{\mathbf{k_0}}\right)$. The incident and scattered wavevectors may be imaginary and therefore in the given formulation, we take into account evanescent waves. We assume that the uniform bidimensional half-plane has an irregular boundary z = h($\mathbf{r}$) at its bottom. The incident field is given by a plane wave of the form:

$$\psi_{in} = q_0^{-1/2} \exp\left(i\mathbf{k_0}.\mathbf{r} + iq_0 z\right) \tag{1}$$

In the region z < min(h($\mathbf{r}$)), the scattered field is written as a superposition of plane waves:

$$\psi_{sc} = \int q_k^{-1/2} S\left(\mathbf{k},\mathbf{k_0}\right) \exp\left(i\mathbf{k}.\mathbf{r} - iq_{\mathbf{k}} z\right) d\mathbf{k} \tag{2}$$

If the wave field is multicomponental, $\psi = \psi_i$, i = 1,...,N, components of electric and magnetic field can be described as ψ_i. The quantity S($\mathbf{k}$,$\mathbf{k_o}$) is called the scattering amplitude (SA). In the case of electromagnetic wave, the scattering amplitude is described by a 2 x 2 matrix. In the following, polarization indexes are omitted. Voronovich's approach is based on the effect of horizontal and vertical translations of the surface profile h($\mathbf{r}$), this leads to a SA of the form:

$$S\left(\mathbf{k},\mathbf{k_0}\right) = \int \exp\left(-i\left(\mathbf{k} - \mathbf{k_0}\right).\mathbf{r} + i\left(q_{\mathbf{k}} + q_{\mathbf{0}}\right)h(\mathbf{r})\right)\Phi\left(\mathbf{k},\mathbf{k_0};\boldsymbol{\xi}\right)e^{i\boldsymbol{\xi}.\mathbf{r}}\, d\mathbf{r}d\boldsymbol{\xi}\big/(2\boldsymbol{\pi})^2 \tag{3}$$

where,

$$\Phi\left(\mathbf{k},\mathbf{k_0};\boldsymbol{\xi}\right) = \delta(\boldsymbol{\xi})\Phi_0\left(\mathbf{k},\mathbf{k_0}\right) + \delta\left(\boldsymbol{\xi} - \boldsymbol{\xi}_1\right)\Phi_1\left(\mathbf{k},\mathbf{k_0};\boldsymbol{\xi}_1\right)h\left(\boldsymbol{\xi}_1\right) + \delta\left(\boldsymbol{\xi} - \boldsymbol{\xi}_1 - \boldsymbol{\xi}_2\right)\Phi_2\left(\mathbf{k},\mathbf{k_0};\boldsymbol{\xi}_1,\boldsymbol{\xi}_2\right)h\left(\boldsymbol{\xi}_1\right)h\left(\boldsymbol{\xi}_2\right) + \ \ldots \tag{4}$$

h($\boldsymbol{\xi}$) is the Fourier transform of the roughness shape:

$$h\left(\boldsymbol{\xi}\right) = \int h(\mathbf{r})\, e^{-i\boldsymbol{\xi}.\mathbf{r}}\, d\mathbf{r}\big/(2\pi)^2 \tag{5}$$

Φ is expanded in a functional Taylor series about $h_o(\boldsymbol{\xi})$ = 0 ($h_o(\boldsymbol{\xi})$ = 0 is the Fourier transform of the flat surface). The functional derivatives in the series are written as function Φ_n to be determined. A final property of Φ_n is:

$$\Phi_n\left(\mathbf{k},\mathbf{k_0};\boldsymbol{\xi}_1,..,\boldsymbol{\xi}_n\right) = 0 \quad \text{if} \quad \text{any} \quad \boldsymbol{\xi}_i\left(i = 1,..,n\right) = \mathbf{0} \tag{6}$$

Following Voronovich, we can define new functions $\widetilde{\Phi}_n$ for n $\geq$ 1 :

$$\Phi_n\left(\mathbf{k},\mathbf{k_0};\boldsymbol{\xi}_1,..,\boldsymbol{\xi}_n\right) = \boldsymbol{\xi}_1..\boldsymbol{\xi}_n\, \widetilde{\Phi}_n\left(\mathbf{k},\mathbf{k_0};\boldsymbol{\xi}_1,..,\boldsymbol{\xi}_n\right) \tag{7}$$

where the $\tilde{\Phi}_n$ are non singular if any $\xi_i(i=1,..,n)=\mathbf{0}$.
(4) becomes then :

$$\Phi(\mathbf{k},\mathbf{k_0};\xi)=\delta(\xi)\tilde{\Phi}_0(\mathbf{k},\mathbf{k_0})+\int \delta(\xi-\xi_1)\tilde{\Phi}_1(\mathbf{k},\mathbf{k_0};\xi_1)\xi_1 h(\xi_1)d\xi_1 + \int \delta(\xi-\xi_1-\xi_2)\tilde{\Phi}_2(\mathbf{k},\mathbf{k_0};\xi_1,\xi_2)\xi_1 h(\xi_1)\xi_2 h(\xi_2)d\xi_1 d\xi_2 + \ldots \quad (8)$$

$\tilde{\Phi}_n$ is bounded at all ξ_1, ξ_2, ... , that is :

$$\left|\tilde{\Phi}_n\right| < A_n \quad (9)$$

Since

$$\int i\xi h(\xi)e^{i\xi.r}d\xi = \nabla h(\mathbf{r}) \quad (10)$$

The successive terms of the series (4) can be estimated as quantities of order $|\nabla h|^n A_n$ where $|\nabla h| << 1$.
Therefore, we have an expansion in small slope. The functions $\tilde{\Phi}_n$ can be determined using a transition to the small perturbation theory.

The expression of the scattering amplitude for small perturbation is given by:

$$S(\mathbf{k},\mathbf{k_0})=V_0(\mathbf{k_0})\delta(\mathbf{k}-\mathbf{k_0})+2i(q_k q_0)^{1/2}B(\mathbf{k},\mathbf{k_0})h(\mathbf{k}-\mathbf{k_0})+(q_k q_0)^{1/2}\int B_2(\mathbf{k},\mathbf{k_0};\xi)h(\mathbf{k}-\xi)h(\xi-\mathbf{k_0})d\xi \quad (11)$$

$V_o(\mathbf{k})$ is the reflection coefficient in specular direction. We consider a perfectly conducting surface, the polarization states are defined as following: the vertically polarized wave is defined when vector **E** lies in the plane of incidence, the horizontally polarized wave is defined vhen vector **H** lies in the plane of incidence and vector **E** is horizontal. **E** is decomposed into two independent directions or polarizations, because there is no component in the direction of propagation **k**. The matrix B is a 2 x 2 matrix. It is defined by:

$$B(\mathbf{k},\mathbf{k_0})=\begin{bmatrix} \dfrac{K^2\mathbf{k}.\mathbf{k_0}-k^2k_0^{\,2}}{q_k q_0 k k_0} & \dfrac{K^2\mathbf{N}.\mathbf{k}\times\mathbf{k_0}}{q_k k k_0} \\ \dfrac{K^2\mathbf{N}.\mathbf{k}\times\mathbf{k_0}}{q_0 k k_0} & -\dfrac{\mathbf{k}.\mathbf{k_0}}{k k_0} \end{bmatrix} \quad (12)$$

B is a general matrix, and **k** may not lie in the plane of incidence : the configuration which is described by the matrix B is a general bistatic one. The matrix B_2 is given by:

$$B_2(\mathbf{k},\mathbf{k_0};\xi)=-2q_\xi B(\mathbf{k},\xi)B(\xi,\xi)B(\xi,\mathbf{k_0}) \quad (13)$$

$\tilde{\Phi}_n$ are determined after expanding the exponent in h in the small slope approximation theory and comparing the result to the small perturbation theory. We obtain the SSA expansion within the accuracy of $(\nabla h)^2$:

$$S(\mathbf{k},\mathbf{k_0})=-\frac{2(q_k q_0)^{1/2}}{Q}\int \exp\left(-i(\mathbf{k}-\mathbf{k_0}).\mathbf{r}+i(q_k+q_0)h(\mathbf{r})\right)\left\{B(\mathbf{k},\mathbf{k_0})-\frac{i}{4}\int M(\mathbf{k},\mathbf{k_0};\xi)h(\xi)e^{i\xi.r}d\xi\right\}d\mathbf{r}/(2\pi)^2 \quad (14)$$

The expression for the matrix $M(\mathbf{k},\mathbf{k_0};\xi)$ is:

$$M(\mathbf{k},\mathbf{k_0};\xi)=B_2(\mathbf{k},\mathbf{k_0};\mathbf{k}-\xi)+B_2(\mathbf{k},\mathbf{k_0};\mathbf{k_0}+\xi)-2QB(\mathbf{k},\mathbf{k_0}) \quad (15)$$

with

$$Q = -(q_k + q_0) \tag{16}$$

3. SCATTERED FIELD INTENSITY

3.1. Bistatic intensity

The scattering surface is defined by its statistical properties, namely the height standard deviation and the related autocorrelation function. In the following both have been considered as Gaussian.

Equation (15) allows calculating the bistatic scattering cross section which is found to be :

$$\Sigma(\mathbf{k},\mathbf{k_0}) = \left(\frac{2q_0 q_k}{Q}\right)^2 \int e^{-i(\mathbf{k}-\mathbf{k_0}).\mathbf{r}}\, R(\mathbf{k},\mathbf{k_0};\mathbf{r})\, d\mathbf{r} \big/ (2\pi)^2 \tag{17}$$

with function $R(\mathbf{k},\mathbf{k_0};\mathbf{r})$ defined as :

$$\begin{aligned} R(\mathbf{k},\mathbf{k_0};\mathbf{r}) = & -e^{-Q^2\sigma^2} \left|B(\mathbf{k},\mathbf{k_0}) - F(\mathbf{k},\mathbf{k_0};\mathbf{0})\right|^2 \\ & + e^{-Q^2(\sigma^2 - W(\mathbf{r}))} \left[\tfrac{1}{16} \int \left|M(\mathbf{k},\mathbf{k_0};\boldsymbol{\xi})\right|^2 S(\boldsymbol{\xi})\, e^{i\boldsymbol{\xi}.\mathbf{r}}\, d\boldsymbol{\xi} \right. \\ & \left. + \left(B(\mathbf{k},\mathbf{k_0}) - F(\mathbf{k},\mathbf{k_0};\mathbf{0}) + F(\mathbf{k},\mathbf{k_0};\mathbf{r})\right)\left(B(\mathbf{k},\mathbf{k_0}) - F(\mathbf{k},\mathbf{k_0};\mathbf{0}) + F(\mathbf{k},\mathbf{k_0};\mathbf{r})\right)^* \right] \end{aligned} \tag{18}$$

σ is the height standard deviation and W ($\mathbf{r}$) is the related autocorrelation function with S (ξ) as Fourier transform, and integral F is defined by :

$$F(\mathbf{k},\mathbf{k_0};\mathbf{r}) = \tfrac{Q}{4} \int M(\mathbf{k},\mathbf{k_0};\boldsymbol{\xi})\, S(\boldsymbol{\xi})\, e^{i\boldsymbol{\xi}.\mathbf{r}}\, d\boldsymbol{\xi} \tag{19}$$

1st and 2nd order solutions are calculated in the following. The contribution of the F function is ignored in the 1st order solution.

3.2. First order solution

The matrix of scattering coefficients is easily obtained for a perfectly conducting material. In the incident plane, these coefficients, derived from the perturbation theory are found to be (12) :

$$\text{TE :} \quad B_{22}(\mathbf{k},\mathbf{k_0}) = -1 \qquad\qquad \text{TM :} \quad B_{11}(\mathbf{k},\mathbf{k_0}) = \frac{K^2 - kk_0}{q_k q_0}$$

for the diagonal terms and :

$$B_{12}(\mathbf{k},\mathbf{k_0}) = 0 \qquad\qquad B_{21}(\mathbf{k},\mathbf{k_0}) = 0$$

for non diagonal terms.

The 1st order solution is obtained ignoring term M (and consequently F). We obtain in this case :

$$R(\mathbf{k},\mathbf{k_0};\mathbf{r}) = \left|B(\mathbf{k},\mathbf{k_0})\right|^2 \left[\exp\left(-Q^2(\sigma^2 - W(\mathbf{r}))\right) - \exp\left(-Q^2\sigma^2\right)\right] \tag{20}$$

This expression is similar to the Kirchhoff approximation. However the geometrical factor is different.

The case of imperfect conductors is more complicated. Details of the calculation are not reproduced in this paper. This case has however been considered and simulation results for the 1st order approximation are reported in the next section.

3.2. Second order solution

TE case

Term $B(\mathbf{k},\mathbf{k_0})$ is equal to -1 for the TE case. $B_2(\mathbf{k},\mathbf{k_0};\boldsymbol{\xi})$ term (see eq. (13) is consequently :

$$B_2(\mathbf{k},\mathbf{k_0};\boldsymbol{\xi}) = 2q_{\boldsymbol{\xi}} \tag{21}$$

and subsequently for M :

$$M(\mathbf{k},\mathbf{k_0};\boldsymbol{\xi}) = 2\left[q_{\mathbf{k}-\boldsymbol{\xi}} + q_{\mathbf{k_0}-\boldsymbol{\xi}} - Q\right] \tag{22}$$

The $F(\mathbf{k},\mathbf{k_0};\mathbf{r})$ integral providing the 2nd order contribution is calculated by FFT.

TM case

M term in this case is :

$$M = -\frac{2}{q_{\mathbf{k}}q_{\mathbf{0}}}\left[\frac{\left[K^2-\mathbf{k}.(\mathbf{k}-\boldsymbol{\xi})\right]\left[K^2-\mathbf{k_0}.(\mathbf{k}-\boldsymbol{\xi})\right]}{q_{\mathbf{k}-\boldsymbol{\xi}}} + \frac{\left[K^2-\mathbf{k}.(\mathbf{k_0}+\boldsymbol{\xi})\right]\left[K^2-\mathbf{k_0}.(\mathbf{k_0}+\boldsymbol{\xi})\right]}{q_{\mathbf{k_0}+\boldsymbol{\xi}}} - Q\left(K^2-\mathbf{k}.\mathbf{k_0}\right)\right] \tag{23}$$

with $q_{\mathbf{k}-\xi} = \left[K^2 - (\mathbf{k}-\xi)^2\right]^{1/2}$ and $q_{\mathbf{k_0}+\xi} = \left[K^2 - (\mathbf{k_0}+\xi)^2\right]^{1/2}$

The first two terms include a singularity. Their calculation is briefly detailed hereafter taking the first one as an example. The integral defined by :

$$\int_{-\infty}^{+\infty} \frac{\left[K^2-\mathbf{k}.(\mathbf{k}-\boldsymbol{\xi})\right]\left[K^2-\mathbf{k_0}.(\mathbf{k}-\boldsymbol{\xi})\right]}{\left[K^2-(\mathbf{k}-\boldsymbol{\xi})^2\right]^{1/2}} S(\boldsymbol{\xi})\ \exp(i\boldsymbol{\xi}.\mathbf{r})\, d\boldsymbol{\xi} \tag{24}$$

which appears in the calculation is singular for K values such that

$$K = \pm|\mathbf{k}-\boldsymbol{\xi}|$$

This singularity is easily removed in both cases of real and complex values of the denominator using convenient changes of integration variables. The integral is then calculated numerically.

The calculation of the term involving the square of modulus of M is more complicated. Corresponding expression is :

$$\int_{-\infty}^{+\infty} \left| \frac{\left[K^2 - \mathbf{k}.(\mathbf{k}-\boldsymbol{\xi})\right]\left[K^2 - \mathbf{k}_0.(\mathbf{k}-\boldsymbol{\xi})\right]}{q_{\mathbf{k}-\boldsymbol{\xi}}} + \frac{\left[K^2 - \mathbf{k}.(\mathbf{k}_0+\boldsymbol{\xi})\right]\left[K^2 - \mathbf{k}_0.(\mathbf{k}_0+\boldsymbol{\xi})\right]}{q_{\mathbf{k}_0+\boldsymbol{\xi}}} - Q\left(K^2 - \mathbf{k}.\mathbf{k}_0\right) \right|^2 S(\boldsymbol{\xi})\ \exp(i\boldsymbol{\xi}.\mathbf{r})\, d\boldsymbol{\xi} \quad (25)$$

The real variable ξ is extended to the complex plane, and the integration is performed in the complex ξ plane. Integration on the real axis from $-\infty$ to 0 is equal to integration from 0 to $+\infty$. Consequently only the second one is considered hereafter.

Jordan lemma applies on a large circle located at infinity provided the autocorrelation function vanishes at infinity. The contour considered is located in the first quadrant. It includes the real axis, a part of a circle at infinity limited to a 45° angular sector due to terms in ξ^2 in the autocorrelation function, and a diagonal to close the contour. The contributions related to the two straight lines are equal. They are calculated numerically on the diagonal which possesses no singularity.

The integral possesses four branch-points for values :

$$q_{\mathbf{k}-\boldsymbol{\xi}} = 0 \qquad \text{and} \qquad q_{\mathbf{k}_0+\boldsymbol{\xi}} = 0$$

The question of inclusion or not of these branch points inside the integration contour relies on their physical meaning. They are on the real axis.

Corresponding waves may be written as $\exp(+i\,q\,h(\mathbf{r}))$:

with $q_{\mathbf{k}-\xi} = \left[K^2 - (\mathbf{k}-\xi)^2\right]^{1/2}$ and $q_{\mathbf{k}_0+\xi} = \left[K^2 - (\mathbf{k}_0+\xi)^2\right]^{1/2}$

Real and imaginary parts of q $\left(q_{real}, q_{imag}\right)$ must be such that term $\exp\left(-iq_{real}h(\mathbf{r}) + q_{imag}h(\mathbf{r})\right)$ vanishes at infinity and corresponds to a progressive wave.

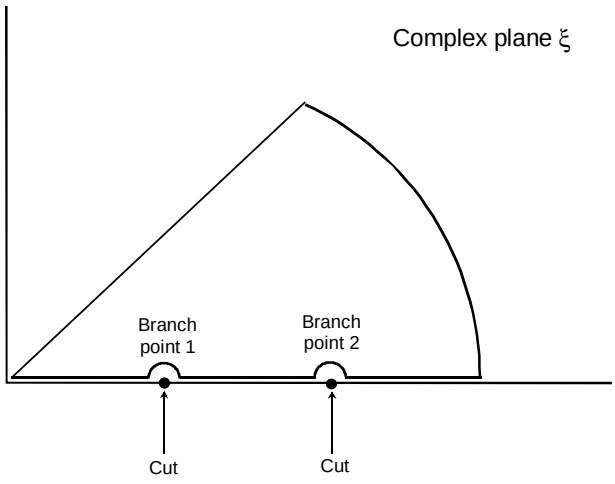

Figure 1: Illustrative example of the integration contour in the complex plane

The choice represented on figure 1 is convenient and brings no additive contribution to the scattered field

4. NUMERICAL SIMULATIONS

Results presented include a comparison between 1st and 2nd order approximations, some comparisons with other published results, cross polarization and backscattering calculations. Calculations have been performed on a square sample considering consequently integration on a surface. Variable θ_i (thetai) is the incidence angle. Its sign is opposite to the sign of the scattering angle, named theta. h is the height standard deviation. L is the height autocorrelation length.

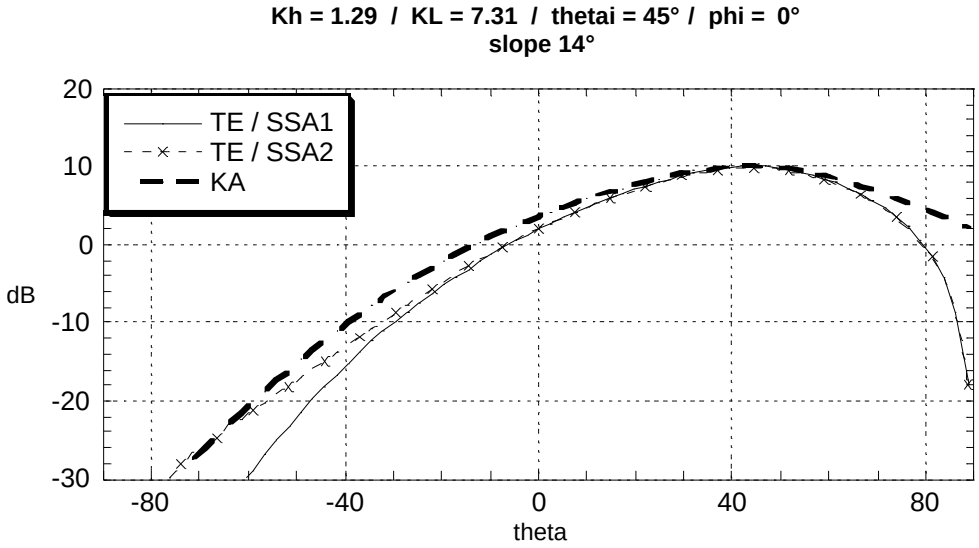

Figure 2 : Comparisons between 1st and 2nd order SSA approximation with Kirchhoff approximation.

SSA 1st and 2nd order results are very close as can be noticed on figure 1 which corresponds to an example already considered by Yang and Broschat[7]. This can be also observed for the TM case and for greater slopes. The results are compared with the Kirchhoff Approximation (KA) result. Peak values are obtained for the specular direction. The results significantly differs when departing from this direction specially for forward scattering at grazing angles.

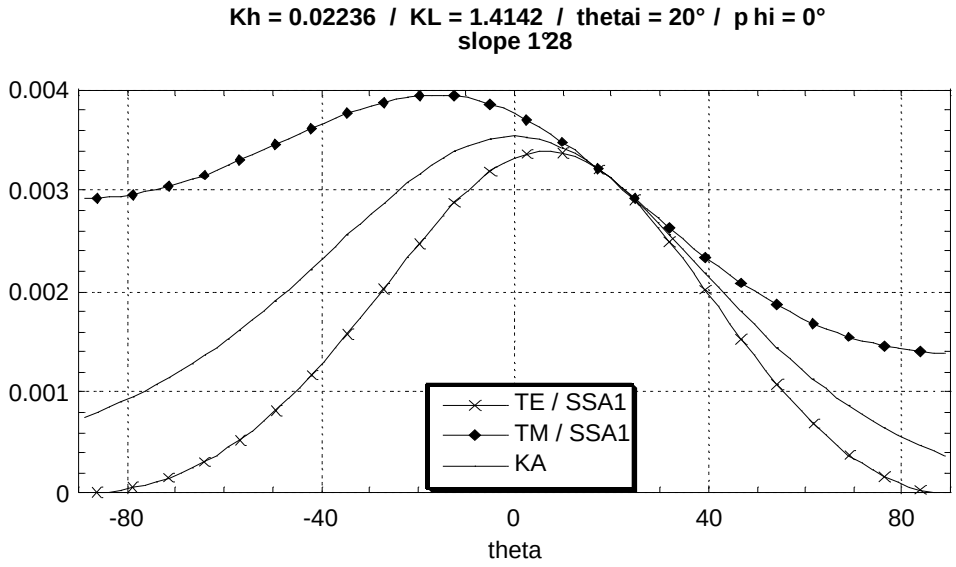

Figure 3 : Comparisons between TE and TM SSA and KA results

The second example (figure 3) corresponds to a case presented by Bahar[6]. Results perfectly agree with those he obtained. The curves merge for the specular direction and depend on the polarization. The polarization dependency does not exist for Kirchhoff Approximation. Only one sign is changed in this last case. The same remarks than in the previous case apply regarding the discrepancies when increasing the scattering angle.

Cross-polarized components calculation modifies the scattering matrix coefficients. The corresponding amplitude vanishes in the plane of incidence and increases with the azimuth angle. Results presented on figure 4 have been obtained considering a 45° angle between incident and scattering planes.

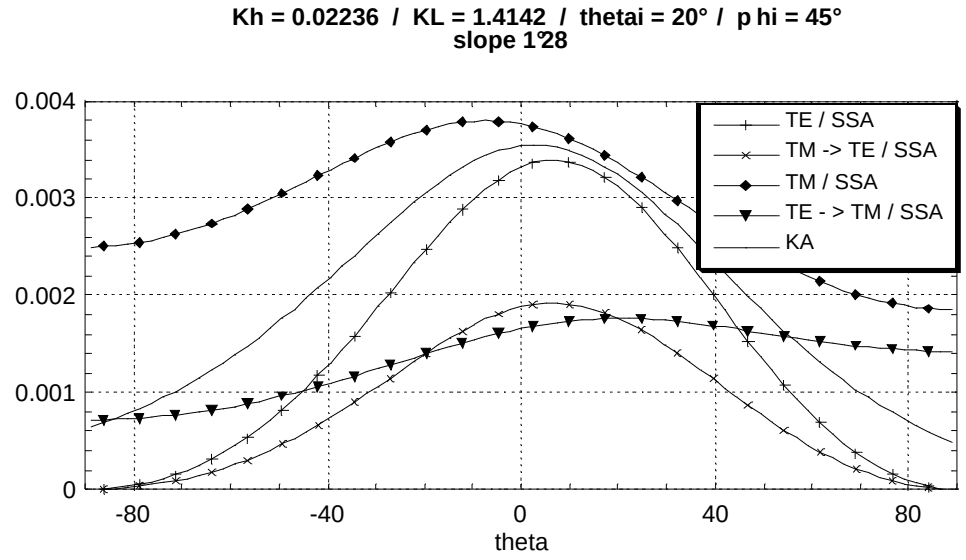

Figure 4 : Cross-polarized terms

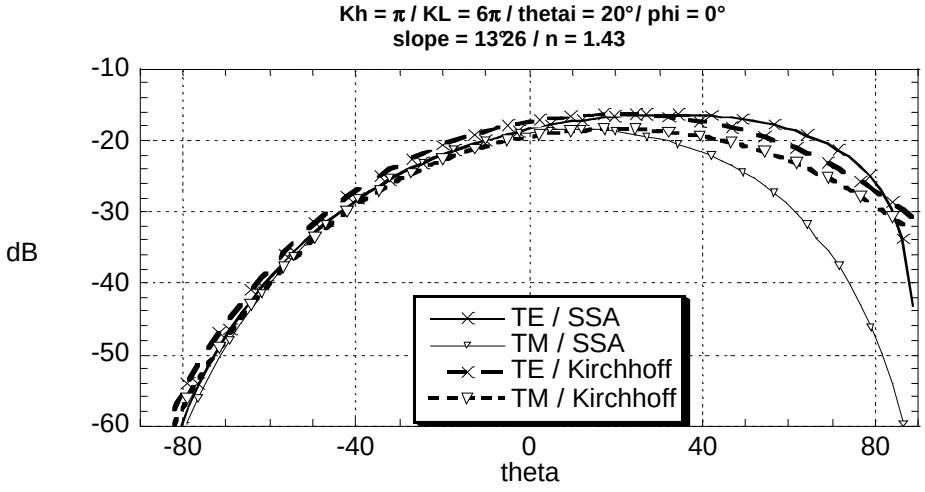

Figure 5 : Scattering by a dielectric rough surface

The results presented on figure 5 applies to the case of dielectric materials. The discrepancies between Kirchhoff approximation and small slope approximation are also significant specially for forward scattering at grazing angles.

5. SCATTERING CROSS-SECTION OF COMPLEX OBJECTS

In this part of the paper we present a method of scattering cross-section calculation for arbitrary complex shaped objects with conducting rough surfaces. The definition we give can be employed for polarized illumination by optical or infrared frequencies and can be extended to laser cross-section. The development of laser radar (ladar) requires modelling softwares to analyze ladar signatures. The first step toward the development of a simulation of ladar signature is an accurate modelling of the interaction of a laser wave with a rough interface because all real surfaces are rough for laser waves. In the previous parts of this paper, we developed a wave scattering theory for randomly rough conducting surfaces based upon Voronovich's Small Slope Approximation. With this theory, a 3-D scattering problem can be resolved and the computation is not time-consuming. Now we discuss the statistical properties of the height standard deviation we have introduced in our calculations. We know that the deviation of a surface from the smooth reference surface is represented by the function h(**r**) of the previous parts. h is the height of the surface from the reference surface and **r** is the position vector on the reference surface. The surface is assumed to be part of a continuous random process which is described by the statistical height distribution p(h). p(h)dh is the probability of any surface point being at a height between h and h + dh. In calculations of scattering from randomly rough conducting surfaces, the height is assumed to be Gaussian. This assumption makes calculations more tractable.

To verify the validity of the Gaussian assumption of surface height fluctuation, we used an atomic force microscope (AFM) with a vertical and horizontal resolution of less than 1 nm, these resolutions are much smaller than the incident wave length of a ladar in the near-infrared band (0.7 to 2 μm), or in the 3- to 5-μm band, or in the 8- to 13-μm band. In this paper, we consider a steel sample. Analysis of AFM picture (Fig. 6) shows that the surface is composed of two roughness regions: a randomly rough region and randomly occuring narrow grooves, pits and sharp tips. Figure 7 shows the distribution of the surface heights of the steel sample. This figure gives evidence for the validity of the assumption that our steel sample possesses a Gaussian distribution for the deviation of the steel surface from the smooth reference. The histogram of the steel surface sample fits well to a Gaussian distribution.

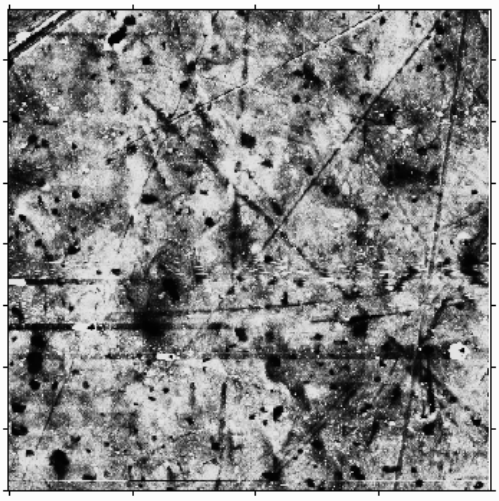

Figure 6 : Atomic force microscope picture of a 40 μm x 40 μm metallic surface

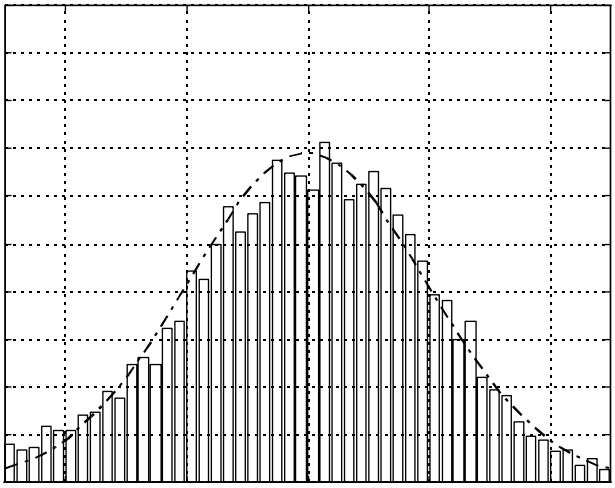

Figure 7 : Description of the height distribution

The detectability of a target under laser illumination may be defined by a laser cross-section (LCS), i.e. an area intercepting the amount of power which, if scattered uniformely in all directions would produce a scattered power density at the receiver equal to that reflected by the target. The laser cross-section is defined by:

$$LCS = (I_r / I_i)\, 4\pi\, r^2 \tag{26}$$

where I_i (watts / sterad) is the intensity incident on the target, I_r (watts / sterad) is the reflected scattered radiant intensity and r is the source to target distance. The laser cross-section is defined in the far-field. Laser illumination is defined by a plane wave. This theoretical analysis of a general 3D conducting rough-scattering configuration is a very difficult problem which can not be solved with a numerical efficient algorithm. We know that the signal scattered by a complex surface contains two components: a specular or coherent component, and a diffuse or incoherent component. In the far-field, for fast detectors, the scattering cross-section is speckle-resolved. However, calculation of the coherent and incoherent components of the scattered electromagnetic field can be simplified in the high frequency limit [8,9,10]. The coherent field component is calculated considering a Kirchhoff based approach in the specular direction. In the case of a monotatic ladar, i.e. the incident direction is equal to the scattered direction, we define a backscattering cross-section which is given for a smooth perfectly conducting object by:

$$\Sigma = \pi\, \rho_1\, \rho_2 \tag{27}$$

where ρ_1 and ρ_2 are the radii of principal curvature of the object surface at the specular reflection point. For a perfectly conducting rough surface, the coherent field may be determined from the average amplitude of the scattered field, the phase of this field is well determined. And this average does not contain the diffuse field. The coherent scattered field is given by the product of the one-dimensional characteristic function of the surface by the field scattered from a smooth surface of the same extent as the rough surface. And the backscattering coherent cross-section for a perfectly conducting object is obtained by:

$$\Sigma_{coherent} = \pi\, \rho_1\, \rho_2\, \chi^2\, (-2\, K) \tag{28}$$

where χ is the one-dimensional characteristic function of the surface, K is the incident wave number.

To determine the diffuse scattered field, it is necessary to consider the mean intensity of the scattered field, because the diffuse field amplitude averages to zero, this is due to the rapidly varying phase of the diffuse field. To compute the backscattering cross-section for the diffuse field, we propose to divide the surface of the perfectly conducting object into planar patches. The dimensions of the patches are much greater than both correlation length and incident wavelength. The incoherent scattering cross-section of a perfectly conducting rough object is given by the superposition of the incoherent backscattering cross-section of each illuminated patch. Multiple scattering from the perfectly conducting surface of the object may be neglected when the radii of the curvature at any point on the surface are much larger than the incident wavelength, the slope of the surface is much smaller than unit. The incoherent intensity scattered by each patch is calculated using the small slope approximation introduced in the previous chapters. The incoherent scattered fields are obtained by the second-order SSA for the vectorial case. The calculation of the incoherent field is performed only over the illuminated region.

6. CONCLUDING REMARKS

We have developped the second-order small slope approximation for the vectorial case and a perfectly conducting two-dimensional surface. The validity of small slope approximation is related only to the smallness of the slopes of the roughness and the small slope approximation is wavelength independent. We have calculated the second order of the small slope approximation to be more accurate for a large range of slopes. We have investigated the singularities of the function M for electromagnetic scattering at a perfectly conducting randomly rough surface and we have obtained the expression of the function in the TE and TM cases. The singularities of the considered function are related to the excitation of surface waves. We have compared the vectorial case of the small slope approximation with Bahar's full-wave approximation and Kirchhoff approximation for two-dimensional conducting surfaces satisfying Gaussian statistics. The SSA gives remarkably accurate results and the averaged expressions for the scattering cross-section are numerically tractable. The SSA is more accurate than Kirchhoff approximation. We have analyzed the backscattering cross-section of arbitrarily shaped perfectly conducting randomly rough surfaces. The formulas of coherent and incoherent backscattering cross-section have been obtained respectively with Kirchhoff approximation and Voronovich's small slope approximation.

ACKNOWLEDGMENTS

The authors are grateful to D. Dubreuil and J. Olivier of Thomson-CSF LCR for the atomic force microscope measurements of the steel sample.

REFERENCES

1. F.G. Bass and I.M. Fuks, *Wave Scattering from Statistically Rough Surfaces,* Academic, New York, 1978.
2. P. Beckmann and A. Spizzichino, *The Scattering of Electromagnetic Waves from Rough Surfaces,* Macmillan, New York, 1963.
3. A.G. Voronovich, *Small Slope Approximation in Wave Scattering by Rough Surface,* Sov. Phys. JETP **62**(1), pp. 65-70, 1985.
4. A.G. Voronovich, *Wave Scattering from Rough Surfaces*, Springer-Verlag, 1995.
5. E. Bahar, G.G. Rajan, *Depolarization and Scattering of Electromagnetic Waves by Irregular Boundaries for Arbitrary Incident and Scatter Angles-Full Wave Solutions,* IEEE Trans. Antennas and Propagation **AP 27**, pp. 214-225, 1979
6. E. Bahar, B.S. Lee, *Radar Scatter Cross Section for Two-Dimensional Random Rough Surfaces-Full Wave solutions and Comparisons with Experiments,* Waves in Random Media **6**, pp. 1-23, 1996.
7. T. Yang, S.L. Broschat, *A Comparison of Scattering Model Results for Two-Dimensional Randomly Rough Surfaces*, IEEE Trans. Antennas and Propagation **AP 40**, pp. 1505-1512, 1992.
8. W. Zhensen and Suomin, *Bistatic Scattering by Arbitrarily Shaped Objects wit Rough Surface at Optical and Infrared Frequencies*, Int. Journal of Infrared and Millimeter Waves Vol. **13, No. 4**, pp. 537-549, 1992.
9. G. Berginc and Y. Béniguel, *Asymptotic Methods for Scattering Cross-Section Calculation of a Rough Surface*, **PIERS Proceedings** Boston, p. 261, 1997.
10. G. Berginc and Y. Béniguel, *Extension of Small-Slope Approximation Method for 3D Scattering Cross-Section Calculation of a Rough Convex Object*, **PIERS Proceedings** Nantes, p.582, 1998.